Na$^+$/K$^+$-pump ligands modulate gating of palytoxin-induced ion channels
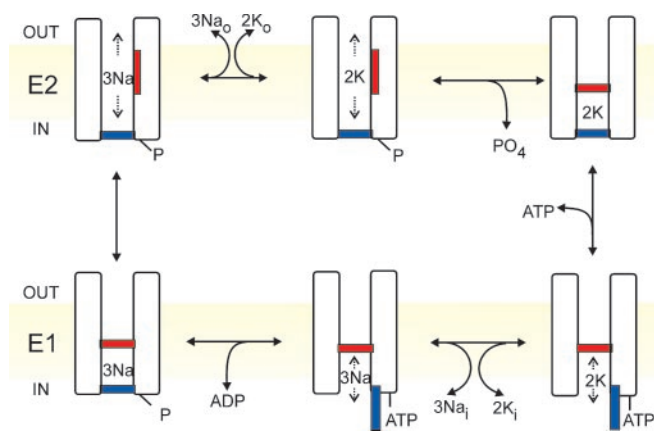
Pablo Artigas and David C. Gadsby*

Laboratory of Cardiac/Membrane Physiology, The Rockefeller University, New York, NY 10021

The Na$^+$/K$^+$ pump is a ubiquitous P-type ATPase that binds three cytoplasmic Na$^+$ ions deep within its core where they are temporarily occluded before being released to the extracellular surface. The 3Na$^+$/2K$^+$-exchange transport cycle is completed when two extracellular K$^+$ ions bind and become temporarily occluded within the protein and subsequently released to the cytoplasm. Coupling of Na$^+$-ion occlusion to phosphorylation of the pump by ATP and of K$^+$-ion occlusion to its dephosphorylation ensure the vectorial nature of net transport. The occluded-ion conformations, with binding sites inaccessible from either side, represent intermediate states in these alternating-access descriptions of transport. They afford protection against potentially catastrophic effects of inadvertently allowing simultaneous access from both membrane sides. The marine toxin, palytoxin, converts Na$^+$/K$^+$ pumps into nonselective cation channels, possibly by disrupting the normal strict coupling between opening of one access pathway in the Na$^+$/K$^+$ ATPase and closing of the other. We show here that gating of the channels in palytoxin-bound Na$^+$/K$^+$ pumps in excised membrane patches is modulated by the pump's physiological ligands: cytoplasmic application of ATP promotes opening of the channels, and extracellular replacement of Na$^+$ ions by K$^+$ ions promotes closing of the channels. This suggests that, despite the presence of bound palytoxin, certain partial reactions of the normal Na$^+$/K$^+$-transport cycle persist and remain capable of effecting the conformational changes that control access to the pump's cation-binding sites. These findings affirm the alternating-access model of ion pumps and offer the possibility of examining ion occlusion/deocclusion reactions in single pump molecules.

Fig. 1. Alternating-gate model of the Post-Albers (9, 10) transport cycle of the Na$^+$/K$^+$ pump represented in cartoon form as a channel with two gates never simultaneously open. Extra- (OUT) and intracellular (IN) surfaces of the membrane (yellow) are indicated, as are E2 states (*Upper*; external gate may open) and E1 states (*Lower*; internal gate may open). Occluded states with both gates shut (*Upper Right*, *Lower Left*) follow binding of 2 external K$^+$, and of 3 internal Na$^+$ and subsequent phosphorylation, respectively. ATP acts with low affinity to speed opening of the internal gate and concomitant K$^+$ deocclusion, and acts with high affinity to phosphorylate the pump.

Although ion-motive pumps and ion channels are both integral membrane proteins that mediate transport of ions across cell membranes, they traditionally have been viewed as very different, largely for kinetic reasons. Thus, up to $\approx 10^8$ ions·s^{-1} flow down their electrochemical gradient through an open channel, whereas a working pump moves only $\approx 10^2$ ions·s^{-1} up their electrochemical gradient. However, this simple comparison ignores the facts that most ion channels spend the majority of their time closed, and that all ion channels contain a gate that is opened and closed by conformational changes that occur on a time scale (milliseconds) similar to those that rate-limit ion pumping (1). Typically, in an ion-motive pump, ions at one membrane surface bind to sites within the protein core and become temporarily occluded there before being deoccluded and released at the opposite surface (2, 3). Thus, an ion pump behaves, at least qualitatively, like an ion channel with two gates, one on each side of the ion-binding cavity, that are constrained to open and close alternately (4–7). The fact that the ion flux through an open ion channel can be as much as 10^6-fold larger than that mediated by an active ion pump dictates that the probability of the pump's hypothetical two gates being open simultaneously must be negligibly small, i.e., $<10^{-6}$, lest the pump fail to effect useful ion transport. Presumably, just as evolution optimized ion-channel structure to maximize conductance while retaining selectivity (8), it optimized the coupling between the gates of ion pumps to preclude open-channel

conformations while facilitating appropriate ligand-mediated gating reactions.

The Na$^+$/K$^+$ pump is a P-type ATPase crucial to the life of practically all animal cells. Its transport cycle, in which three Na$^+$ ions are extruded from the cell and two K$^+$ ions are recovered, at the expense of one molecule of ATP, is cartooned in Fig. 1 as a sequence of steps that alternates access to ion binding sites within an ion channel (4–7). The pump adopts two principal conformations, E1 with the binding sites accessible from the cytoplasm (Fig. 1 *Lower*), and E2 with access from the extracellular space (Fig. 1 *Upper*). Binding of the third cytoplasmic Na$^+$ to E1 triggers phosphorylation (denoted "**P**", Fig. 1 *Lower Left*) of the pump from ATP, acting with high apparent affinity (≤ 1 μM), and concomitant occlusion of the 3 Na$^+$, so trapping them within the pump (11). Spontaneous relaxation to the E2 conformation opens the external gate, allowing release of the Na$^+$ to the exterior followed by binding of 2 extracellular K$^+$ (Fig. 1 *Upper Left*); the latter promotes occlusion of the K$^+$ ions (2, 3) and dephosphorylation of the pump (Fig. 1 *Upper Right*). Subsequent binding of ATP, with relatively low apparent affinity (≈ 100 μM), speeds the conformational change of the dephos-
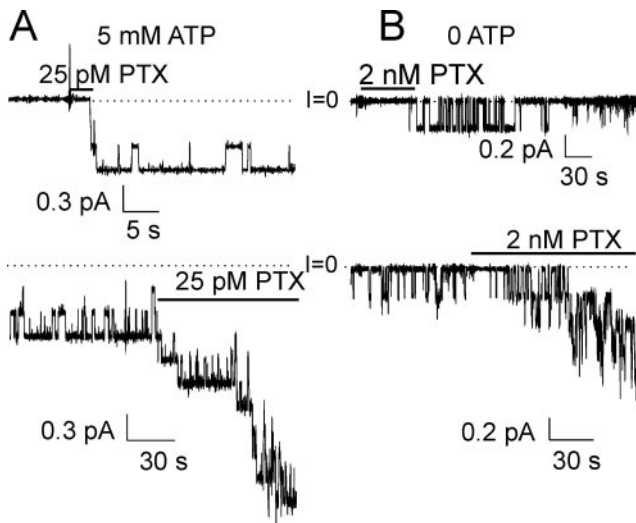
Fig. 2. ATP increases P_o of PTX-induced channels in outside-out patches from myocytes, bathed by ≈150 mM Na solutions and held at −40 mV; dotted lines mark zero current (I = 0). (*A Upper*) With 5 mM internal ATP three channels were activated (within ≈4 s) by 25 pM PTX; the channels gated with high P_o after PTX withdrawal. (*Lower*) Continuation of the top record showing gating of the same channels for a longer period, and opening of more channels after reapplication of PTX. (*B Upper*) Without pipette ATP, 2 nM PTX elicited (within ≈60 s) opening of one channel, which showed low P_o after PTX removal (P_o = 0.19 ± 0.04, n = 4; from patches with apparently only one channel recorded for >4 min after PTX washout). (*Lower*) Continued gating of the same channel in absence of PTX (12 min of record omitted), and increase in the number active channels (still with low P_o) after PTX readdition.

phorylated pump, E2→E1, which opens the internal gate and releases the K^+ into the cytoplasm (Fig. 1 *Lower Right*). In contrast to the high-affinity, phosphorylating action of ATP, its

low-affinity binding effect is mimicked by ADP (12, 13), and by poorly hydrolyzable ATP analogs (14).

Although mutagenesis experiments (e.g., ref. 15) and the high-resolution crystal structures of the related P-type Ca^{2+}-ATPase (16, 17) have begun to suggest likely sites for coordination of the bound cations deep within this and homologous pumps, the locations, structures, and mechanisms of the gates in any ion-motive pump remain unknown. To begin addressing these questions in the Na^+/K^+ pump, we have exploited the lethal toxin, palytoxin (PTX), isolated from marine coelenterates of the genus *Palythoa* (18). PTX has been shown to bind to the Na^+/K^+ pump (18–20), and to somehow cause appearance of nonselective cation channels (21) that likely usurp at least some portion of the pump's intrinsic ion translocation pathway (22, 23). We examined, in excised patches, changes in the gating of PTX-induced channels in the Na^+/K^+ pump in response to addition or removal of ATP, or of Na^+ and K^+ ions, at the cytoplasmic or external membrane surface, respectively. Our results show that, despite the presence of a tightly bound PTX molecule, the inner and outer gates of the Na^+/K^+ pump can still be regulated by the pump's physiological ligands. This implies that the Na^+/K^+ pump (and, by extension, other ion-motive pumps) may legitimately be considered as an ion channel with two gates that are normally never open simultaneously (4–7), and suggests an experimental approach to examining the locations and structures of those gates.

Materials and Methods

Currents were recorded at 22–25°C in outside-out or inside-out excised membrane patches (24) using an Axopatch 200B amplifier and PCLAMP7 software (Axon Instruments, Inc.) for data acquisition and analysis. The patches were excised from guinea-pig ventricular myocytes (isolated as described; ref. 25) or from HEK293 cells (from ATCC) seeded on polylysine-coated coverslips in Petri dishes 1–3 days before recordings. Thin-walled borosilicate glass pipettes were coated with Sylgard and had
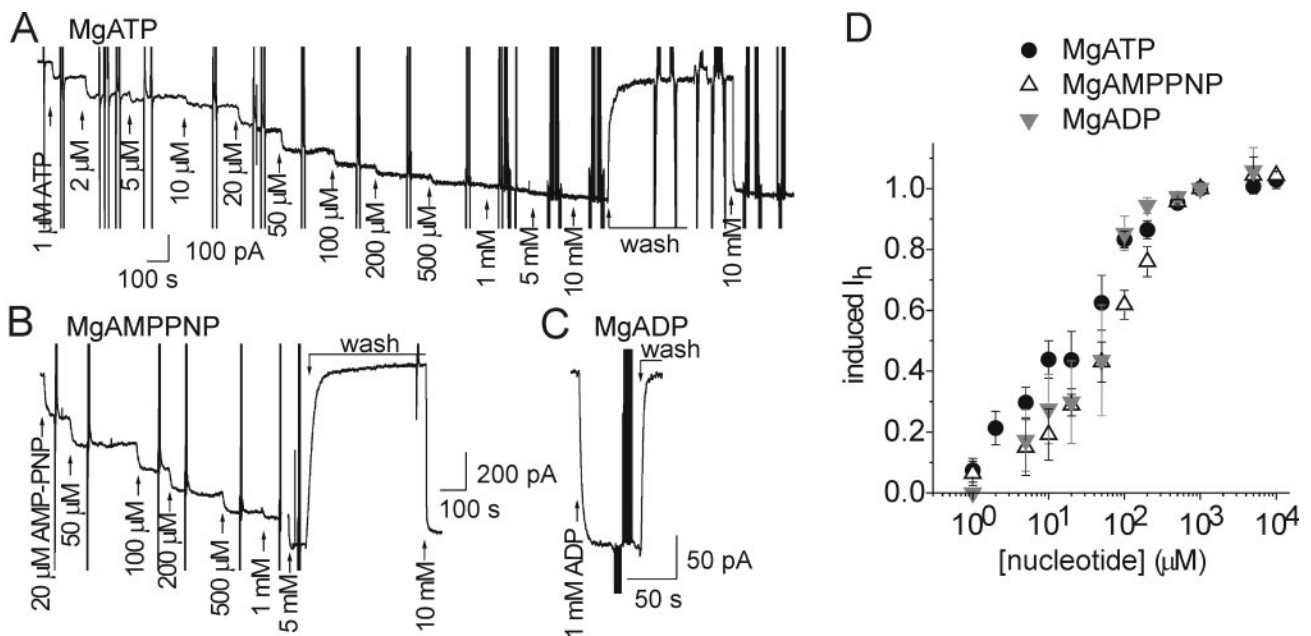
Fig. 3. ATP, AMPPNP, and ADP similarly enhance PTX-induced current in inside-out patches from HEK293 cells held at −20 mV, and bathed in ≈150 mM Na^+ solutions, with 100 nM PTX in the pipette. (*A*) Increasing [MgATP] at the cytoplasmic surface progressively augmented macroscopic current; large vertical deflections reflect collection of conductance data. (*B*) Comparable influence of MgAMPPNP recorded from a different patch. (*C*) Effect of addition and removal of 1 mM MgADP. (*D*) Dose-response curves for current enhancement by all three nucleotides. Least squares fits (omitted for clarity) to the Hill equation yielded parameters: for ATP (black circles), K_{ATP} = 21 ± 3 μM, n_H = 0.8 ± 0.1 (n = 4); for AMPPNP (open triangles), K_{AMPPNP} = 59 ± 6 μM, n_H = 1 ± 0.1 (n = 3); for ADP (gray inverted triangles) K_{ADP} = 37 ± 4 μM, n_H = 1 ± 0.1 (n = 3).

resistances of 2–8 MΩ for macroscopic, and 15–30 MΩ for microscopic, current recording. The extracellular solution contained (in mM): 140 sulfamic acid, 10 Hepes, 10 HCl, 1 MgCl$_2$, 1 CaCl$_2$, 0.5 BaCl$_2$, and 160 mM Na$^+$, K$^+$, or Cs$^+$. [BaCl$_2$] was increased to 5 mM in the experiments of Fig. 5 A and B to enhance block of endogenous K$^+$-channels. The intracellular (pipette) solution for outside-out patches was (in mM): 150 Na$^+$, 130 L-glutamic acid, 10 Hepes, 10 EGTA, 10 TEACl, with or without nucleotide as specified in the figure legends; in intracellular solutions for inside-out patches 145 mM sulfamic acid replaced glutamic acid, and [EGTA] was 0.5 mM. MgATP, Na$_2$ADP, or Li$_4$AMPPNP were added from 200 mM stock solutions (pH 7.4 with NMDG), and equimolar MgCl$_2$ was added together with ADP and AMPPNP. All solutions had a pH of 7.4 and osmolality of 285–305 mOsm kg^{-1}. An aliquot of 100 μM PTX (*Palythoa toxica*, Calbiochem) stock solution (in H$_2$O) was defrosted and diluted into external solutions just before each experiment; all such PTX-containing solutions also included 0.002% BSA to minimize PTX binding to nonglass surfaces.

Results and Discussion

With saturating, 5 mM, internal (intrapipette) MgATP, and $\approx$150 mM Na$^+$ at both membrane surfaces, brief exposure of an outside-out excised membrane patch containing native Na$^+$/K$^+$ pumps to only 25 pM PTX quickly activated 3 channels (Fig. 2A *Upper*), all of which remained active with a high open probability (P_o, fraction of time spent open = 0.93 $\pm$ 0.02; SEM, $n = 3$) after withdrawal of unbound PTX (Fig. 2A *Lower*; *cf.* Fig. 4A, below). Subsequent reapplication of the same low [PTX] to the same patch activated several more channels, all of which also displayed a high P_o (Fig. 2A *Lower*). In contrast, without internal ATP, a longer application of a much higher [PTX] (2 nM) to a similar patch elicited only one evident channel (Fig. 2B *Upper*), which continued opening and closing minutes after PTX washout (Fig. 2B *Lower*) but with low P_o (0.19 $\pm$ 0.04, $n = 4$); reapplication of the 2 nM PTX again induced more channels and these showed comparably low P_o.

As these different patterns of channel opening and closing long after washout of PTX cannot reflect toxin binding and unbinding reactions, we conclude that ATP must modulate the gating of channels with PTX still bound to them. To see whether this ATP effect resulted from high-affinity phosphorylation of the pump protein or low-affinity binding to the pump, we measured the dependence on [MgATP] of the increase in macroscopic current (flowing through thousands of pump channels) in inside-out excised patches with saturating [PTX] (100 nM) in the 160-mM Na$^+$-containing solution present at the extracellular surface (inside the pipette) (Fig. 3). MgATP acted with low apparent affinity to increase the current (Fig. 3 A and D), suggesting that nucleotide binding to the E2 state (Fig. 1) underlies the ATP-induced increase in both P_o in single-channel recordings, and macroscopic current in patches with many pump channels. In keeping with this interpretation, the poorly hydrolyzable MgAMPPNP (Fig. 3B), and MgADP (Fig. 3C), similarly increased PTX-induced current (6- $\pm$ 1-fold; $n = 8$ for MgATP; $n = 6$ for MgAMPPNP; $n = 4$ for MgADP), with apparent affinities like that for MgATP (Fig. 3D). Because unbinding of PTX under these conditions takes tens of minutes (e.g., Fig. 4, below), the rapid increases and decreases in current (within seconds) upon addition and withdrawal of nucleotide must reflect changes in open probability (i.e., in gating) of PTX-bound pump channels. This stabilization by nucleotides of the open state of PTX-induced channels (Figs. 2 and 3) shares characteristics of the low-affinity ATP binding believed responsible for opening the Na$^+$/K$^+$ pump's internal gate during the normal, 3 Na$^+$ outward:2 K$^+$ inward, ion transport cycle (Fig. 1).

Because binding of extracellular K$^+$ ions leads to their occlusion in the Na$^+$/K$^+$ pump (3, 12), and so may be expected to
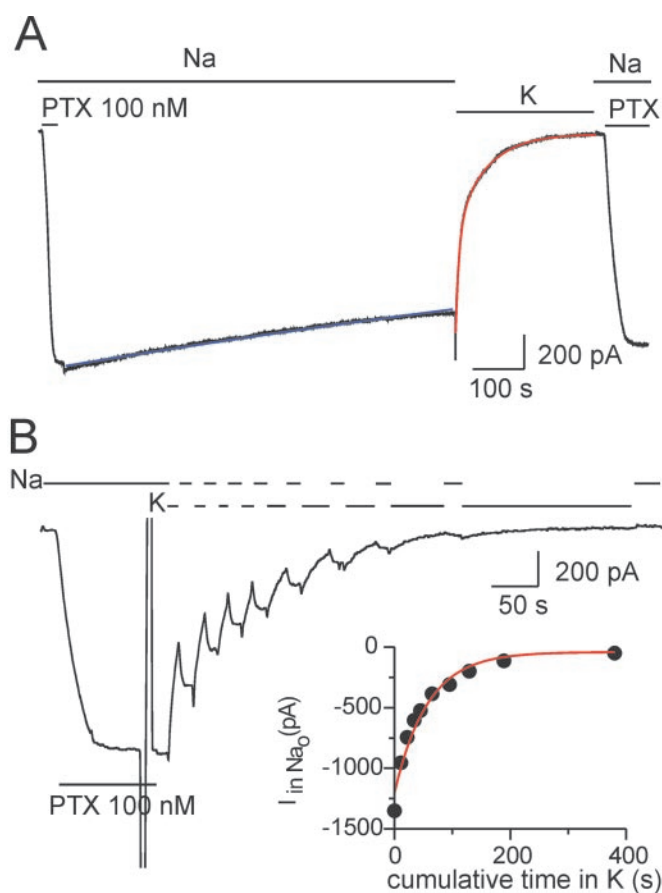
Fig. 4. External K$^+$ closes PTX-induced channels in an outside-out HEK293 patch, held at -20 mV, in the absence of ATP. (*A*) After activation by 100 nM PTX, macroscopic current decline upon PTX withdrawal in external Na$^+$ was slow ($\tau = 2600$ s; blue fit line), but was accelerated upon replacing 160 mM Na$^+$ with 160 mM K$^+$ (double exponential fit, red line, gives A$_f$ = A$_s$ = 0.5, τ_f = 8 s, and τ_s = 61 s). Returning to Na$^+$ after 300 s in K$^+$ was without effect until PTX was reapplied. (*B*) Distinction between closing and PTX unbinding in the same patch as in *A*; brief substitution of K$^+$ for Na$^+$ produced rapid, partially reversible, current decay. (*Inset*) Rate of PTX unbinding in K$^+$ estimated from the plot of residual current amplitude in Na$^+$ solution against cumulative time spent in K$^+$ (exponential fit, red line, yields $\tau = 57$ s).

promote closing of its external gate, we tested the influence of external K$^+$ (or its congener Cs$^+$) on the P_o of PTX-induced channels. In the absence of internal (in the pipette) ATP, addition of 100 nM PTX to an outside-out patch in 160-mM Na$^+$-containing external solution promptly elicited a large macroscopic current, which decayed extremely slowly ($\tau = 1671 \pm 369$ s, $n = 5$) after withdrawal of the PTX (Fig. 4A). But, sudden replacement of all external Na$^+$ by K$^+$ dramatically (after a small instantaneous increase that reflects faster permeation of K$^+$ through the channels; *cf.* ref. 26) accelerated current decay, which followed a biexponential time course (red fit line; with fast and slow time constants $\tau_f = 9 \pm 2$ s, and $\tau_s = 50 \pm 9$ s; $n = 10$). Switching back to Na$^+$ solution did not restore the current (Fig. 4A *Right*) until PTX was reapplied, indicating that the PTX had completely unbound during the $\approx$300-s exposure to K$^+$-containing PTX-free solution. To distinguish mere channel closure from PTX unbinding, we greatly abbreviated each exposure to K$^+$, interrupting the current decay with brief switches back to the Na$^+$-containing (but PTX-free) external solution (Fig. 4B) to assay the fraction of pump channels to which PTX had remained bound (Fig. 4B *Inset*). The partial restoration of current during each reexposure to Na$^+$-containing solution
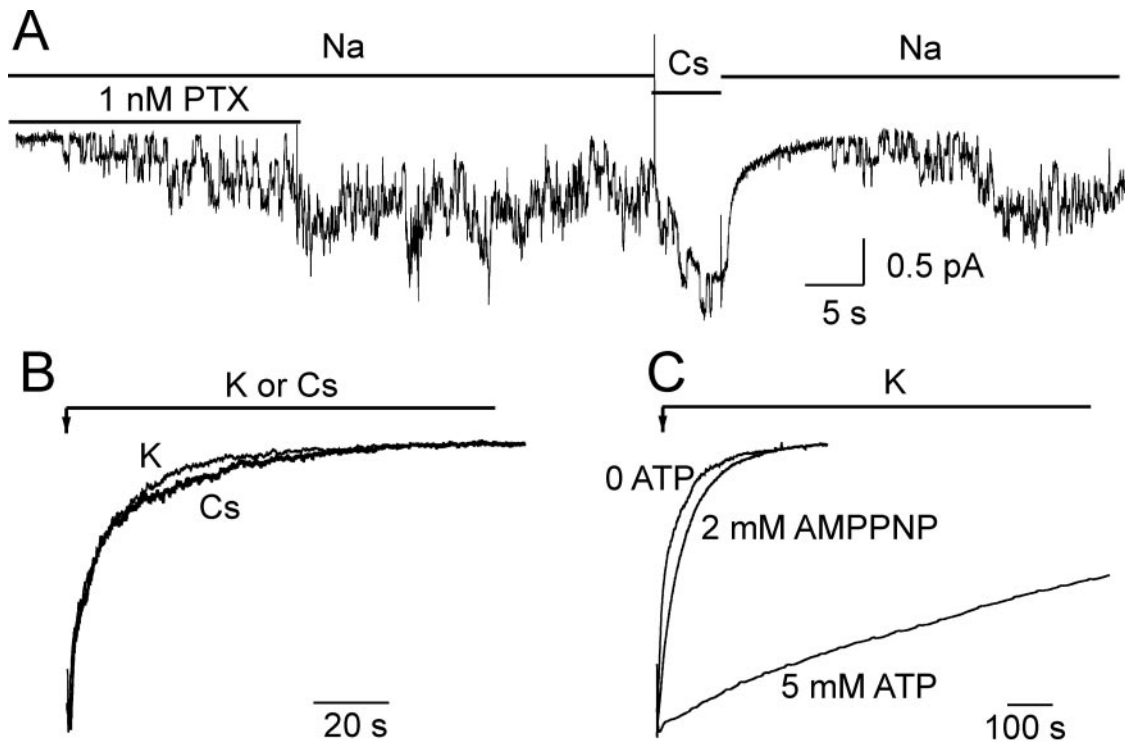
Fig. 5. (*A*) The K$^+$ congener Cs$^+$ closes PTX-induced channels in an outside-out myocyte patch held at -40 mV, bathed by Na$^+$ solutions but with no internal ATP. The few channels activated by 1 nM PTX remained active after PTX washout until replacement of 160 mM external Na$^+$ by 160 mM Cs$^+$ quickly reduced the P_o to ≈ 0. Channels slowly reopening to the initial current level after reapplication of Na$^+$ indicates that PTX did not unbind; the ≈ 1-pA baseline shift on switching to and from Cs$^+$ solution is an artifact due to the change of seal current. (*B*) After brief application of 200 nM PTX in 160 mM Na$^+$ solution (not shown) to the same patch as in *A*, 160 mM Cs$^+$ (thick trace) or 160 mM K$^+$ (thin trace) elicited rapid decay of the 200- to 250-pA current with similar time courses. (*C*) Influence of pump phosphorylation on closing of PTX-induced channels by 160 mM K$^+$. Normalized current traces from three outside-out patches from HEK293 cells with or without pipette nucleotide as indicated. After brief exposure to 100 nM PTX in Na$^+$ (not shown), switching to K$^+$ promoted channel closing that was fast without nucleotide (0 ATP trace) or with 2 mM MgAMPPNP, but very slow with 5 mM MgATP.

(Fig. 4*B*), long after withdrawal of PTX, must reflect the reopening by Na$^+$ ions of PTX-bound channels that had been temporarily closed by K$^+$. Accordingly, plotting the size of the residual current measured in Na$^+$ solution against the cumulative time spent until then in K$^+$ (Fig. 4*B Inset*) yields the time constant for PTX unbinding in the K$^+$ solution, which averaged 56 ± 17 s ($n = 6$).

The fast closing of PTX-bound channels by external K$^+$ or Cs$^+$ is shown directly in Fig. 5. At least four channels in an outside-out patch, activated by 1 nM PTX in Na$^+$-containing external solution (but with no nucleotide in the pipette), continued gating after washout of the PTX (as expected from the macroscopic current record in Fig. 4*A*). But, near the end of the 5-s exposure to Cs$^+$ solution (the reversible ≈ 1-pA baseline current shift reflects a Cs$^+$ vs. Na$^+$ difference in pipette seal current) only single channel openings could be seen (Fig. 5*A*); indeed, during the initial few seconds after removing Cs$^+$ and restoring Na$^+$ solution, no channel openings were seen at all. However, the channel activity soon reappeared in the sustained presence of Na$^+$, despite the continued absence of PTX from the solution (Fig. 5*A*). This indicates that most, if not all, of the pump channels still had PTX tightly bound to them, and that the Cs$^+$ ions had temporarily held them in a closed state. This result with Cs$^+$ is the microscopic correlate of the events illustrated in Fig. 4*B*, in which K$^+$ ions acted on thousands of pump channels. That K$^+$ and Cs$^+$ act comparably under these conditions is confirmed by the closely similar time courses of (normalized) macroscopic current relaxation in Fig. 5*B*, reflecting the closing of thousands of channels (in the same patch as in Fig. 5*A*), after opening them with saturating [PTX] (200 nM) in Na$^+$-

containing solution, and then suddenly switching to either K$^+$ or Cs$^+$ solution.

It is well known that occlusion of K$^+$ prompts dephosphorylation of the pump (2), and that phosphorylation of the pump with inorganic phosphate and Mg^{2+}, by reversal of normal dephosphorylation steps, releases occluded K$^+$ to the extracellular solution (27). This implied antagonism between the influence of external K$^+$ ions and of phosphorylation status on the disposition of the pump's external gate likely underlies the marked slowing of the K$^+$-induced decay of pump-channel current we observed when 5 mM MgATP was included in the intracellular solution (Fig. 5*C*). Thus, after activating large macroscopic currents with 100 nM PTX in outside-out patches exposed to Na$^+$-containing solutions, the usual rapid current relaxation, reflecting channel closing, was seen upon sudden replacement of external Na$^+$ by K$^+$ when there was no nucleotide in the internal solution (Fig. 5*C*, 0 ATP trace), but the decay was slowed >100-fold by 5 mM internal MgATP (5 mM ATP trace; $\tau = 2109 \pm 275$ s, $n = 5$). This effect must be ascribed to phosphorylation of the pump by ATP, rather than to ATP binding at the low affinity site, because inclusion of 2 mM MgAMPPNP in the intracellular solution slowed channel closing by K$^+$ hardly at all (Fig. 5*C*, 2mM AMPPNP trace).

These results strongly suggest that in the presence of PTX the Na$^+$/K$^+$ pump behaves like an ion channel with two gates, one accessible from the extracellular side and the other accessible from the cytoplasmic side, whose opening and closing are regulated by interactions with the pump's principal physiological ligands. That the effects of PTX are fully reversible and repeatable (Fig. 4*A*), and that the P_o (i.e., gating) of PTX-induced

Artigas and Gadsby

channels can be systematically varied by alterations in the external [Na$^+$] and [K$^+$] (Figs. 4 and 5), internal [nucleotide] (Figs. 2 and 3), and/or phosphorylation status (Fig. 5C), argues that PTX neither permanently nor grossly distorts the Na$^+$/K$^+$ pump structure. Also, in PTX-treated Na$^+$/K$^+$ pumps, cysteine scanning mutagenesis of two membrane-spanning helices (22, 23) that, on the basis of point mutation studies (e.g., ref. 15) and comparisons with the Ca^{2+}-ATPase crystal structure (16, 17), are believed to contribute to the lining of the Na$^+$/K$^+$ pump's normal ion translocation pathway, suggests that the pore of the PTX-induced channels includes at least part of that pathway. Moreover, in unmodified native Na$^+$/K$^+$ pumps a short-lived ion channel-like state, remaining closed at the cytoplasmic end but open to the extracellular solution, has been proposed to conduct at least the first of the three released Na$^+$ ions to the exterior following their deocclusion (28–31). Channel-like states have also been inferred responsible for apparently electrodiffusive ion flows observed under certain conditions in native Na$^+$/K$^+$ pumps (ref. 32, but *cf.* ref. 33), and also in native Ca^{2+}-ATPases of surface (34) and sarcoplasmic reticular (35) membranes; the small flows in the latter case are consistent with an average channel P_o on the order of 10^{-8}, compatible with our expectation ($<10^{-6}$) for a functioning pump. Finally, a briefly opening "flickering gate" has been proposed (27) to limit movement of K$^+$ and its congeners between their binding sites in the (unmodified) Na$^+$/K$^+$ pump and the extracellular solution.

The possibility arises, therefore, that an overall channel-related architecture and alternating-gate transport mechanism may be general features of ion-motive P-type ATPases. For the PTX-induced channel in the Na$^+$/K$^+$ pump, our demonstration of substrate-modulated gating events that at least qualitatively mimic those that accompany ion occlusion and deocclusion during normal Na$^+$/K$^+$ transport by the unmodified pump, suggests that we may use PTX to investigate, at the level of single pump molecules, the molecular mechanisms of the conformational changes associated with ion occlusion and deocclusion. This will entail analyses of variations in single-channel gating kinetics with substrate concentrations, as well as cysteine-scanning studies of accessibility of residues along the ion translocation pathway under different gating conditions. Such approaches should yield structural insights into the molecular movements that control active ion transport by ion-motive pumps.

1. Hille, B. (2001) *Ion Channels of Excitable Membranes* (Sinauer, Sunderland, MA).
2. Post, R. L., Hegyvary, C. & Kume, S. (1972) *J. Biol. Chem.* **247,** 6530–6540.
3. Beaugé, L. A. & Glynn, I. M. (1979) *Nature* **280,** 510–512.
4. Patlak, C. S. (1957) *Bull. Math. Biophys.* **19,** 209–235.
5. Vidaver, G. A. (1966) *J. Theor. Biol.* **10,** 301–306.
6. Jardetzky, O. (1966) *Nature* **211,** 969–970.
7. Läuger, P. (1979) *Biochim. Biophys. Acta* **552,** 143–161.
8. Morais-Cabral, J. H., Zhou, Y. & MacKinnon, R. (2001) *Nature* **414,** 37–42.
9. Post, R., Sen, A. M. & Rosenthal, A. S. (1965) *J. Biol. Chem.* **240,** 1437–1445.
10. Albers, R. W. (1967) *Annu. Rev. Biochem.* **36,** 727–756.
11. Glynn, I. M., Hara, Y. & Richards, D. E. (1984) *J. Physiol. (London)* **351,** 531–547.
12. Glynn, I. M. & Richards, D. E. (1982) *J. Physiol. (London)* **330,** 17–43.
13. Kaplan, J. H. & Kenney, L. J. (1982) *Ann. N.Y. Acad. Sci.* **402,** 292–295.
14. Simons, T. J. B. (1975) *J. Physiol. (London)* **244,** 731–739.
15. Pedersen, P. A., Nielsen, J. M., Rasmussen, J. H. & Jorgensen, P. L. (1998) *Biochemistry* **37,** 17818–17827.
16. Toyoshima, C., Nakasako, M., Nomura, H. & Ogawa, H. (2000) *Nature* **405,** 647–655.
17. Toyoshima, C. & Nomura, H. (2002) *Nature* **418,** 605–611.
18. Habermann, E. (1989) *Toxicon* **27,** 1171–1187.
19. Scheiner-Bobis, G., Meyer zu Heringdorf, D., Christ, M. & Habermann, E. (1994) *Mol. Pharmacol.* **45,** 1132–1136.
20. Redondo, J., Fiedler, B. & Scheiner-Bobis, G. (1996) *Mol. Pharmacol.* **49,** 49–57.
21. Muramatsu, I., Nishio, M., Kigoshi, S. & Uemura, D. (1988) *Br. J. Pharmacol.* **93,** 811–816.
22. Guennoun, S. & Horisberger, J. D. (2000) *FEBS Lett.* **482,** 144–148.
23. Guennoun, S. & Horisberger, J. D. (2002) *FEBS Lett.* **513,** 277–281.
24. Hamill, O. P., Marty, A., Neher, E., Sakmann, B. & Sigworth, F. J. (1981) *Pflügers Arch.* **391,** 85–100.
25. Gadsby, D. C. & Nakao, M. (1989) *J. Gen. Physiol.* **94,** 511–537.
26. Tosteson, M. T., Halperin, J. A., Kishi, Y. & Tosteson, D. C. (1991) *J. Gen. Physiol.* **98,** 969–985.
27. Forbush, B. (1988) *Prog. Clin. Biol. Res.* **268A,** 229–248.
28. Gadsby, D. C., De Weer, P. & Rakowski, R. F. (1993) *Science* **260,** 100–103.
29. Hilgemann, D. W. (1994) *Science* **263,** 1429–1433.
30. Wuddell, I. & Apell, H. J. (1995) *Biophys. J.* **69,** 909–921.
31. Holmgren, M., Wagg, J., Bezanilla, F., Rakowski, R. F., DeWeer, P. & Gadsby, D. C. (2000) *Nature* **403,** 898–901.
32. Wang, X. & Horisberger, J. D. (1995) *Am. J. Physiol.* **37,** C590–C595.
33. Rettinger, J. (1996) *Biochim. Biophys. Acta* **1282,** 207–215.
34. Antoine, S., Pinet, C. & Coulombe, A. (2001) *J. Membr. Biol.* **179,** 37–50.
35. de Meis, L. & Inesi, G. (1992) *FEBS Lett.* **299,** 33–35.